pISSN 2384-1095
eISSN 2384-1109

iMRI 2015;19:146-152

http://dx.doi.org/10.13104/imri.2015.19.3.146

iMRI
Investigative Magnetic Resonance Imaging

Associated Brain Parenchymal Abnormalities in Developmental Venous Anomalies: Evaluation with Susceptibility-weighted MR Imaging

Hyeon Gyu Ryu[1], Dae Seob Choi[1,2], Soo Bueum Cho[1], Hwa Seon Shin[1], Ho Cheol Choi[1], Boseul Jeong[1], Hyemin Seo[1], Jae Min Cho[1]

[1]Department of Radiology and Gyeongsang National University School of Medicine, Jinju, Korea
[2]Gyeongsang Institute of Health Science, Gyeongsang National University School of Medicine, Jinju, Korea

Original Article

Received: July 12, 2015
Revised: August 15, 2015
Accepted: August 18, 2015

Correspondence to:
Dae Seob Choi, M.D.
Department of Radiology, Gyeongsang National University Hospital, Gyeongsang National University School of Medicine, 90 Chilam-dong, Jinju 660-702, Korea.
Tel. +82-55-750-8211
Fax. +82-55-758-1568
Email: choids@gnu.ac.kr

Purpose: The purpose of this study was to evaluate the associated brain parenchymal abnormalities of developmental venous anomalies (DVA) with susceptibility-weighted image (SWI).

Materials and Methods: Between January 2012 and June 2013, 2356 patients underwent brain MR examinations with contrast enhancement. We retrospectively reviewed their MR examinations and data were collected as per the following criteria: incidence, locations, and associated parenchymal signal abnormalities of DVAs on T2-weighted image, fluid-attenuated inversion recovery (FLAIR), and SWI. Contrast enhanced T1-weighted image was used to diagnose DVA.

Results: Of the 2356 patients examined, 57 DVAs were detected in 57 patients (2.4%); 47 (82.4%) were in either lobe of the supratentorial brain, 9 (15.7%) were in the cerebellum, and 1 (1.7%) was in the pons. Of the 57 DVAs identified, 20 (35.1%) had associated parenchymal abnormalities in the drainage area. Among the 20 DVAs which had associated parenchymal abnormalities, 13 showed hemorrhagic foci on SWI, and 7 demonstrated only increased parenchymal signal abnormalities on T2-weighted and FLAIR images. In 5 of the 13 patients (38.5%) who had hemorrhagic foci, the hemorrhagic lesions were demonstrated only on SWI.

Conclusion: The overall incidence of DVAs was 2.4%. Parenchymal abnormalities were associated with DVAs in 35.1% of the cases. On SWI, hemorrhage was detected in 22.8% of DVAs. Thus, we conclude that SWI might give a potential for understanding of the pathophysiology of parenchymal abnormalities in DVAs.

Keywords: Cerebral developmental venous anomaly; Hemorrhage; MR; Susceptibility-weighted imaging (SWI)

INTRODUCTION

Developmental venous anomalies (DVAs) of the brain are frequently encountered on contrast-enhanced (CE) CT or MR imaging. They are regarded as normal variants of the cerebral venous development and are usually asymptomatic (1-4). However, it has been reported that MR signal abnormalities in the adjacent brain parenchyma could be

associated with DVAs (5, 6). Venous congestion or infarction due to stenosis, or occlusion of the collecting vein, may cause parenchymal signal abnormalities in the drainage area of a DVA (1, 2, 5, 6). Sometimes, a DVA can also be associated with a cavernous angioma (CA), also referred to as a mixed angioma. CAs are usually manifested as hemorrhagic foci. When DVAs are associated with CAs, they can also show parenchymal signal abnormalities due to the hemorrhagic lesions of the CAs (7-10).

Susceptibility-weighted imaging (SWI) is a highly sensitive MR sequence for the detection of hemorrhage (11-14). Recent reports show that SWI is more sensitive in detecting hemorrhagic foci in CAs than the T2-weighted and conventional gradient echo (GRE) images (15). However, there have been few reports in which authors have used SWI for the evaluation of parenchymal signal abnormalities in DVAs (16). If we can find more hemorrhagic lesions in DVAs, it would help us to better understand the pathophysiology of parenchymal signal abnormalities associated with DVAs. The purpose of this study was to evaluate the associated brain parenchymal abnormalities of DVAs with SWI.

MATERIALS AND METHODS

Patient Population

This retrospective study was approved by our Institutional Review Board. Informed consent was waived.

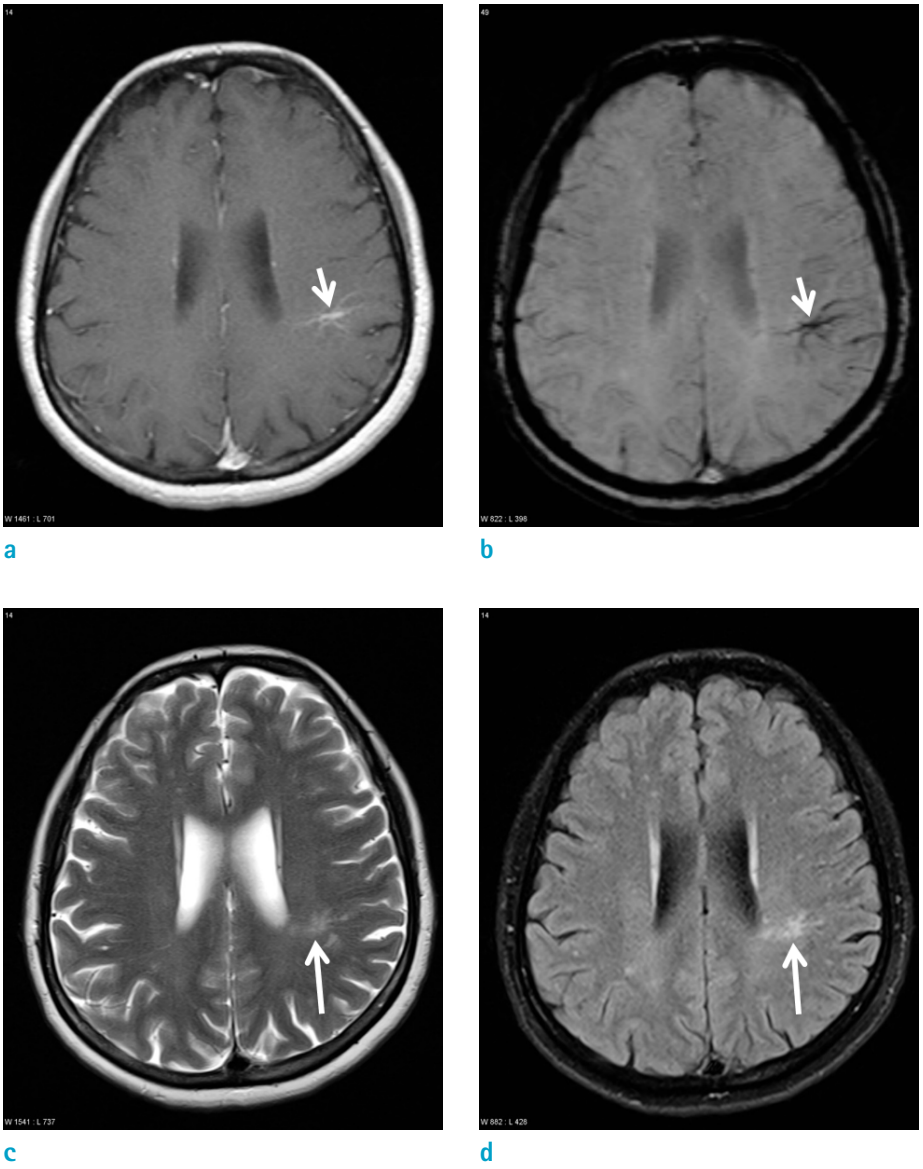

Fig. 1. A 55-year-old female with a DVA. Enhanced T1-weighted image (a) and SWI (b) show a DVA in the left parietal lobe (short arrows). T2-weighted (c) and FLAIR (d) images reveal parenchymal signal abnormalities in and around the DVA (long arrows).

From January 2012 to June 2013, 2356 consecutive patients underwent brain MR examinations with SWI and CE study. A retrospective review of their MR imaging identified DVAs in 57 patients (2.4%) on CE T1-weighted images. There were 32 male and 25 female patients, aged 19 to 92 years (mean, 59.1 years). The criteria used to establish the diagnosis of DVA are based on MR imaging findings, especially on CE T1-weighted images. DVAs are characterized by a cluster of venous radicles that converge into a collecting vein, resulting in the typical 'caput medusae' appearance (Figs. 1-3).

MR Imaging

All MR examinations were performed on a 1.5 Tesla (T) MR scanner (MagnetomAvanto, Siemens Medical solution, Erlangen, Germany). Our MR protocol consisted of T2-weighted imaging, fluid-attenuated inversion recovery (FLAIR), SWI, T1 and CE T1-weighted imaging (Table 1). SWI was acquired using a full velocity-compensated, three-dimensional, GRE sequence having the following parameters: repetition time (TR) = 48 ms; echo time (TE) = 40 ms; flip angle (FA) = 15; bandwidth = 80 kHz; slice thickness = 2 mm, with 64 slices in a single slab; matrix size = 256 × 168. The acquisition time was 3 minutes and 7 seconds, with the use of iPAT factor 2. All images were obtained in the same axial plane. Subsequently, 2-mm minIP images were generated. The sequence, along with the entire image processing, was automated on a Siemens MR scanner platform. The SWI and minIP images were uploaded and made available on the picture archiving and communication (PACS) system.

Image Analysis

The MR examinations were reviewed in detail by two

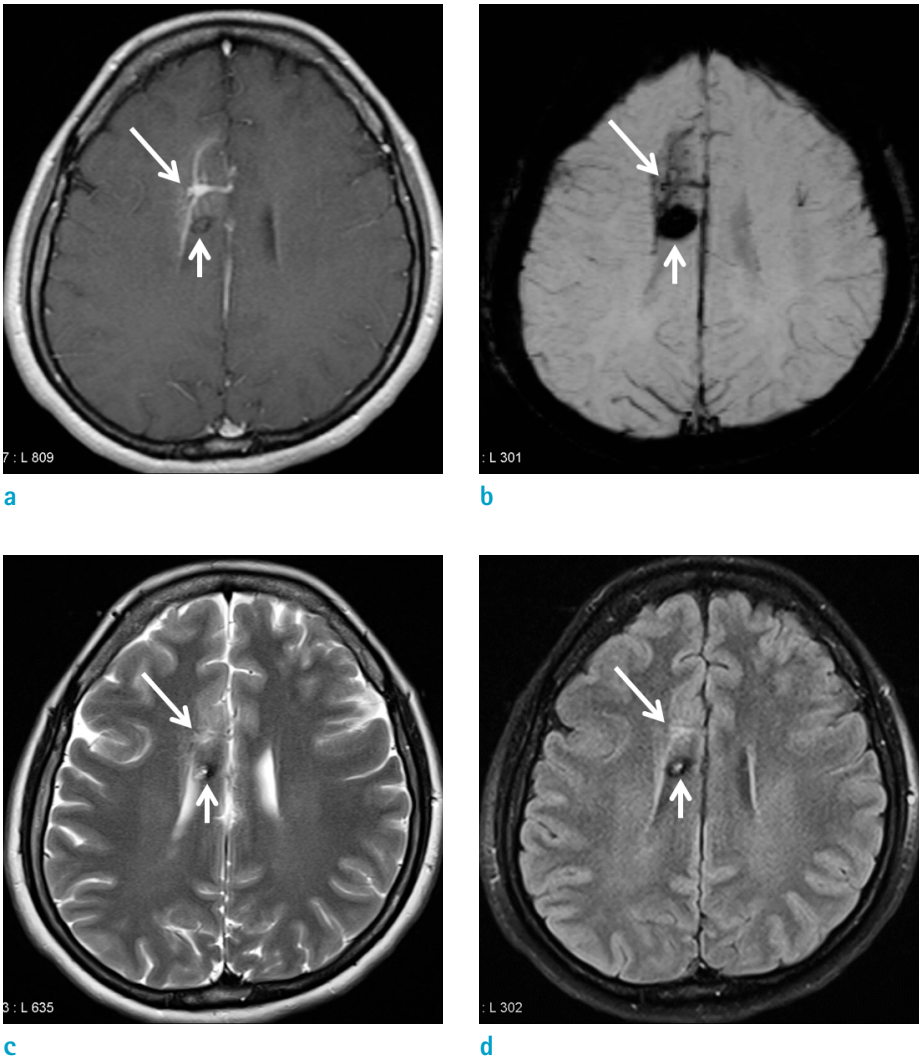

Fig. 2. A 36-year-old female with a DVA. Enhanced T1-weighted (a), SWI (b), T2-weighted (c) and FLAIR (d) images show a DVA (long arrows) and an associated hemorrhagic lesion (short arrows) in the right frontal lobe and corpus callosum. Both the DVA and hemorrhagic lesion are more conspicuously demonstrated on SWI than on T2-weighted and FLAIR images.

radiologists. One radiologist had an added qualification in neuroradiology and 15 years' experience in evaluating brain MR imaging; the other radiologist had three years of experience interpreting and assessing MR images. Data were collected with respect to the following: the location of DVA, the associated increased signal intensity, and the associated hemorrhage in the drainage area of DVA on FLAIR, T2-weighted images, and SWI. The drainage territory was defined as the brain parenchyma directly adjacent to the visualized radicles of the DVA. Signal intensity

Table 1. MR Imaging Protocol

Sequence	Repetition time (msec)	Echo time (msec)	Field of view (mm)	Matrix	Section thickness (mm)	Intersection gap	Imaging time
T2	4300	98	220	384 × 209	5	2	1 min 6 sec
FLAIR	8000	117	220	256 × 186	5	2	2 min 10 sec
SWI	48	40	220	256 × 168	2	0	3 min 7 sec
T1	552	17	220	256 × 128	5	2	1 min 14 sec
Enhanced T1	552	17	220	256 × 128	5	2	1 min 14 sec

FLAIR = fluid-attenuated inversion recovery; SWI = susceptibility-weighted image; T1 = T1-weighted image; T2 = T2-weighted image

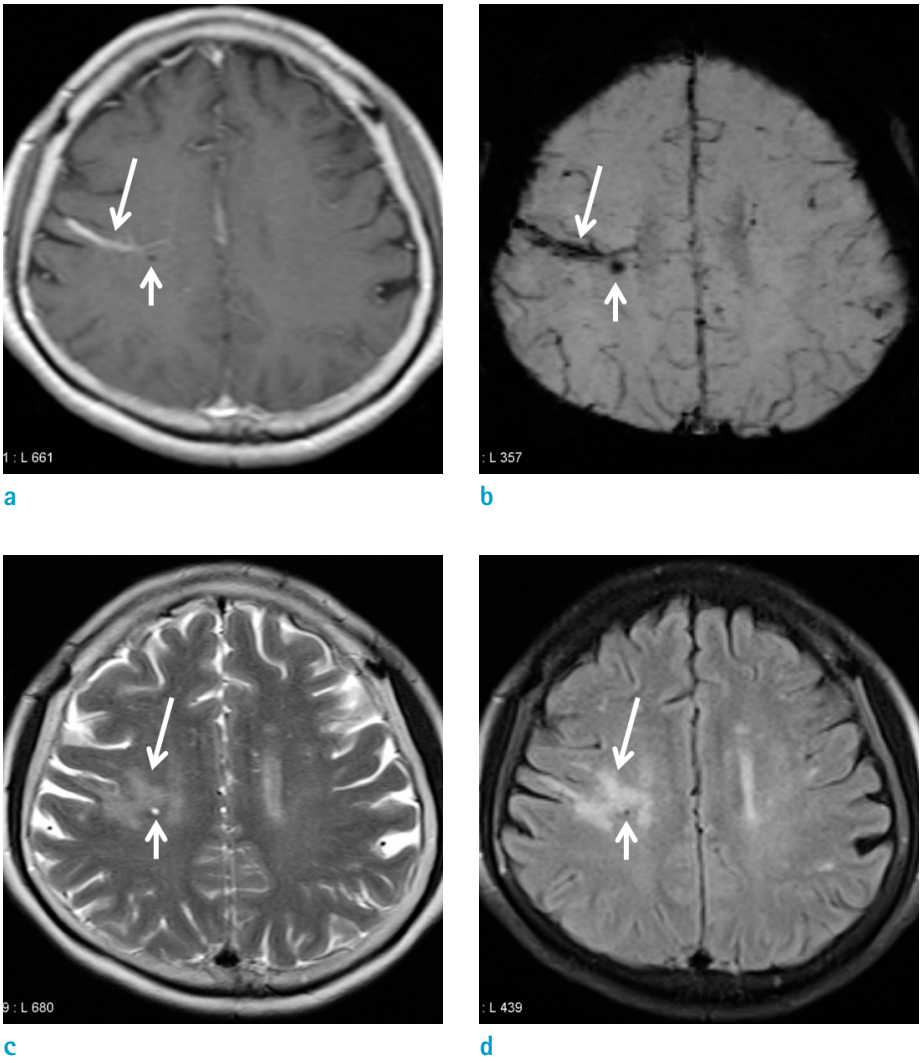

a b c d

Fig. 3. A 59-year-old female with a DVA. Enhanced T1-weighted image (a) and SWI (b) show a DVA in the right frontoparietal lobe (long arrows). There is also a focal hemorrhagic lesion on SWI (short arrows). T2-weighted (c) and FLAIR (d) images demonstrate hyperintense signal abnormalities in the drainage territory of the DVA (long arrows). The hemorrhagic lesion is seen as a focal cystic lesion (short arrows).

alterations adjacent to the DVA were defined as increased extravascular signal intensities within the directly subjacent brain parenchyma. We were careful not to include signal intensity within the visible vascularity of the DVA, as commonly identified on FLAIR imaging. Imaging findings were determined by consensus of both the radiologists.

RESULTS

Of the 2356 patients examined, we identified 57 DVAs in 57 patients (2.4%). Based on their location, 47 DVAs (82.4%) were in either lobe of the supratentorial brain, 9 (15.7%) were in the cerebellum, and 1 (1.7%) was in the pons.

Of the 57 DVAs identified, 20 (35.1%) had associated parenchymal abnormalities in the drainage area (Table 2) (Figs. 1-3). Among the 20 DVAs having associated parenchymal abnormalities, 13 (65%) showed hemorrhagic foci on SWI (Figs. 2, 3) and 7 (35%) demonstrated only increased parenchymal signal abnormalities on T2-weighted and FLAIR images (Fig. 1). In 5 (38.5%) of the 13 patients who had hemorrhagic foci, the hemorrhagic lesions were demonstrated only on SWI (Fig. 3). In the remaining 8 patients, although both T2-weighted images and SWI showed the hemorrhagic foci as signal void lesions, they were more prominently demonstrated on SWI than on T2-weighted images (Fig. 2).

Table 2. Patients with Parenchymal Abnormalities Associated with Developmental Venous Anomalies

Patients	Age/sex	Symptoms or clinical indications	Locations	Hemorrhage on SWI
1	53/M	Seizure	L occipital	X
2	78/M	Tremor	R parietal	O
3	71/F	Meningitis	R insula	X
4	61/F	Meningioma follow-up	R occipital	O
5	55/F	Headache	L parietal	X
6	87/F	Dementia	R frontal	O
7	55/M	Parkinson's disease	L frontal	X
8	77/F	Dizziness	R parietal	O
9	46/M	Numbness	R frontal	X
10	27/M	Anxiety	R frontal	X
11	63/F	Dizziness	R parietal	O
12	59/F	Hemiparesis	R parietal	O
13	43/F	ICH	Pons	O
14	72/F	Meningitis	L frontal	O
15	42/M	SAH	R frontal	O
16	36/F	Dizziness	R frontal	O
17	43/F	ICH	L frontal	O
18	65/M	Hemianopsia	L parietal	X
19	65/M	TGA	R frontal	O
20	42/F	Colon cancer	R frontal	O

ICH = intracerebral hemorrhage; L = left; R = right; SAH = subarachnoid hemorrhage; SWI = susceptibility-weighted image; TGA = transient global amnesia

DISCUSSION

Cerebral vascular malformations are classified into four categories: arteriovenous malformation, capillary telangiectasia, DVA, and CA (1, 2). Of these, DVA is the most common, with a 2.6% incidence seen in 4069 brain autopsies (3). In our study, DVAs were demonstrated in 57 (2.4%) of the 2356 patients, which is similar the previous reports (3, 4).

In the present study, parenchymal signal abnormalities were associated in 20 (35.1%) of the 57 DVAs. Previous reports have been variable for the incidence of parenchymal signal abnormalities associated with DVAs (5, 6, 16, 17), ranging from 12.5% to 54.1%. The reason for this variability may be related to differences in the patient population, inclusion and exclusion criteria, and sample size. Different machines and scanning parameters of the studies may also be a factor.

Venous hypertension due to thrombosis or stenosis of the collecting vein is the underlying mechanism leading to symptomatic infarction or asymptomatic parenchymal signal abnormalities in DVAs (1, 2, 5, 6). In cases of no demonstrable stenosis, partial thickening of the veins forming the DVA may also contribute to the development of venous hypertension, by reducing the size and compliance of the vessel lumen, increasing the resistance to flow, and diminishing the vessel's capacity to adapt to pressure modifications (1). In a recent study that evaluated diffusion and perfusion-weighted MR imaging in patients with parenchymal signal abnormalities associated with DVAs, the signal abnormalities around DVAs showed increased ADC, increased cerebral blood volume, and delayed mean transit time and time-to-peak, as opposed to those of the contralateral normal portions. They concluded that the parenchymal signal abnormalities associated with DVAs were caused by vasogenic edema with congestion and

delayed perfusion (17).

In the past, DVAs were thought to be rare lesions that were associated with intracerebral hemorrhage (18, 19). Since the advent of MR imaging, it has been reported that DVAs were relatively prevalent and were associated with a relative risk of hemorrhage. The hemorrhagic lesions associated with DVAs are attributed to coexistent CAs. However, they may also be caused by venous infarction secondary to DVA thrombosis in the absence of a coexisting CA (1).

SWI is a high-spatial resolution, three dimensional, GRE MR technique, which maximizes sensitivity to magnetic susceptibility effects (13, 14). Deoxygenated blood products (deoxyhemoglobin, methemoglobin, and hemosiderin), being paramagnetic with four unpaired electrons, generates magnetic fields that are additively combined with the external magnetic field (13, 14, 20). SWI uses paramagnetic deoxyhemoglobin in the cerebral vein as an intrinsic contrast agent; this is useful for the demonstration of the cerebral venous anatomy (13, 21). Because DVA is a normal variation of the transmedullary vein, it usually shows similar flow velocity and deoxyhemoglobin concentration as the normal cerebral vein. On SWI, DVA is demonstrated as a signal void lesion with the normal cerebral veins. In our study, SWI was useful for the demonstration of DVA itself as well as associated hemorrhage (Figs. 1-3). Among the 13 patients who had hemorrhagic foci, 5 (38.5%) showed the hemorrhagic lesions only on SWI (Fig. 3). In the remaining 8 patients, although both T2-weighted images and SWI showed the hemorrhagic foci as signal void lesions, they were more prominently demonstrated on SWI than on T2-weighted images (Fig. 2).

In our study, hemorrhagic foci were detected in 13 (22.8%) of the 57 DVAs on SWI (Table 2) (Figs. 2, 3). In a recent study of Takasugi et al. (16), hemorrhagic lesions were observed in 62.3% of DVAs on SWI. The discrepancy in our results and those of Takasugi et al. (16) might be due to several factors. First, our patients were scanned using a 1.5T MR machine, whereas Takasugi's group used a 3T scanner. Susceptibility effect in higher field strength increases the conspicuity of paramagnetic substances. Second, the method of patient selection was different. We retrospectively reviewed all brain MR examinations which were undertaken during the study period. However, they selected their patients from the data base of MR imaging reports. In a routine clinical practice, it tends to be that a subtle, small, or uncomplicated incidental DVA might not be mentioned in a MR imaging report, which might work as a selection bias.

In conclusion, the incidence of DVAs was 2.4%, having associated parenchymal abnormalities in 35.1% of the cases. On SWI, hemorrhage was detected in 22.8% of DVAs. We are of the opinion that SWI might give a potential for understanding the pathophysiology of parenchymal abnormalities in DVAs.

REFERENCES

1. Ruiz DS, Yilmaz H, Gailloud P. Cerebral developmental venous anomalies: current concepts. Ann Neurol 2009;66:271-283
2. San Millan Ruiz D, Gailloud P. Cerebral developmental venous anomalies. Childs Nerv Syst 2010;26:1395-1406
3. Sarwar M, McCormick WF. Intracerebral venous angioma. Case report and review. Arch Neurol 1978;35:323-325
4. Garner TB, Del Curling O Jr, Kelly DL Jr, Laster DW. The natural history of intracranial venous angiomas. J Neurosurg 1991;75:715-722
5. Santucci GM, Leach JL, Ying J, Leach SD, Tomsick TA. Brain parenchymal signal abnormalities associated with developmental venous anomalies: detailed MR imaging assessment. AJNR Am J Neuroradiol 2008;29:1317-1323
6. San Millan Ruiz D, Delavelle J, Yilmaz H, et al. Parenchymal abnormalities associated with developmental venous anomalies. Neuroradiology 2007;49:987-995
7. Wilms G, Bleus E, Demaerel P, et al. Simultaneous occurrence of developmental venous anomalies and cavernous angiomas. AJNR Am J Neuroradiol 1994;15:1247-1254; discussion 1255-1257
8. Huber G, Henkes H, Hermes M, Felber S, Terstegge K, Piepgras U. Regional association of developmental venous anomalies with angiographically occult vascular malformations. Eur Radiol 1996;6:30-37
9. Abe T, Singer RJ, Marks MP, Norbash AM, Crowley RS, Steinberg GK. Coexistence of occult vascular malformations and developmental venous anomalies in the central nervous system: MR evaluation. AJNR Am J Neuroradiol 1998;19:51-57
10. Uchino A, Hasuo K, Matsumoto S, et al. Cerebral venous angiomas associated with hemorrhagic lesions. Their MRI manifestations. Clin Imaging 1996;20:157-163
11. Sehgal V, Delproposto Z, Haacke EM, et al. Clinical applications of neuroimaging with susceptibility-weighted imaging. J Magn Reson Imaging 2005;22:439-450
12. Tong KA, Ashwal S, Obenaus A, Nickerson JP, Kido D, Haacke EM. Susceptibility-weighted MR imaging: a review of clinical applications in children. AJNR Am J Neuroradiol

2008;29:9-17
13. Tsui YK, Tsai FY, Hasso AN, Greensite F, Nguyen BV. Susceptibility-weighted imaging for differential diagnosis of cerebral vascular pathology: a pictorial review. J Neurol Sci 2009;287:7-16
14. Haacke EM, Mittal S, Wu Z, Neelavalli J, Cheng YC. Susceptibility-weighted imaging: technical aspects and clinical applications, part 1. AJNR Am J Neuroradiol 2009;30:19-30
15. de Souza JM, Domingues RC, Cruz LC Jr, Domingues FS, Iasbeck T, Gasparetto EL. Susceptibility-weighted imaging for the evaluation of patients with familial cerebral cavernous malformations: a comparison with t2-weighted fast spin-echo and gradient-echo sequences. AJNR Am J Neuroradiol 2008;29:154-158
16. Takasugi M, Fujii S, Shinohara Y, Kaminou T, Watanabe T, Ogawa T. Parenchymal hypointense foci associated with developmental venous anomalies: evaluation by phase-sensitive MR Imaging at 3T. AJNR Am J Neuroradiol 2013;34:1940-1944
17. Jung HN, Kim ST, Cha J, et al. Diffusion and perfusion MRI findings of the signal-intensity abnormalities of brain associated with developmental venous anomaly. AJNR Am J Neuroradiol 2014;35:1539-1542
18. Saito Y, Kobayashi N. Cerebral venous angiomas: clinical evaluation and possible etiology. Radiology 1981;139:87-94
19. Senegor M, Dohrmann GJ, Wollmann RL. Venous angiomas of the posterior fossa should be considered as anomalous venous drainage. Surg Neurol 1983;19:26-32
20. Thomas B, Somasundaram S, Thamburaj K, et al. Clinical applications of susceptibility weighted MR imaging of the brain - a pictorial review. Neuroradiology 2008;50:105-116
21. Haacke EM, Xu Y, Cheng YC, Reichenbach JR. Susceptibility weighted imaging (SWI). Magn Reson Med 2004;52:612-618